Long-term CEP-stable high energy few-cycle pulses using the feed-forward method

Fabian Lücking[*a,b], Alexandria Anderson[a], Alexander Apolonski[b],
Ferenc Krausz[b], Günter Steinmeyer[c], Gabriel Tempea[a], Andreas Assion[a]
[a]Femtolasers Produktions GmbH, Fernkorngasse 10, 1100 Vienna, Austria
[b]Ludwig-Maximilians-Universität München, Am Coulombwall 1, 85748 Garching, Germany
[c]Max-Born-Institut für Nichtlineare Optik und Kurzzeitspektroskopie,
Max-Born-Straße 2a, 12489 Berlin, Germany

ABSTRACT

The feed-forward technique has recently revolutionized carrier-envelope phase stabilization, enabling unprecedented values of residual phase jitter. Nevertheless, in its original demonstrations the stabilized beam exhibited angular and temporal dispersion. We demonstrate that these problems can be solved, resulting in few-cycle pulses with good beam quality. This in turn enables the use of monolithic interferometers, providing excellent long-term stability of the system. Out-of-loop RMS phase noise of less than 80 mrad over 33 minutes (0.5 mHz to 5 kHz) is measured, i.e., a value that has previously been reported for a few seconds integration time. The current method promises to enable reliable operation of CEP-stable systems over several days.

Keywords: Carrier-envelope phase stabilization, feed-forward method, frequency combs, self-referencing, few-cycle pulses, attosecond science

1. INTRODUCTION

1.1 Conventional CEP stabilization

When Ti:Sapphire laser pulses reached the few-cycle barrier, the significance of the carrier-envelope phase (CEP) and its relation to the to the frequency comb spectrum of a mode-locked laser was realized for the first time[1]. Ever since, the rapid progress in both attosecond science and frequency metrology has been steadily increasing the requirements on CEP or comb offset stabilization. As long as suitable sources for attosecond and high-field experiments remain limited to kHz repetition rates, two factors are crucial to successful measurements. First, the precision of the CEP control determines the reproducibility of shot-to-shot experiments, e.g., the spectral and temporal shape of the attosecond XUV pulses generated in a gas target. A second often underestimated aspect is the long-term stability of the CEP lock. Due to the low efficiency of such highly nonlinear processes, many experiments in attosecond physics demand long integration times and tolerate no drop-outs over hours or days of operation. The conventional approach to CEP stabilization[2,3] is to lock the carrier-envelope offset (CEO) frequency f_{CE} of the oscillator to the n-th fraction of the repetition rate f_{rep} ,such that the pulse-to-pulse phase slip

$$\Delta\Phi = \frac{2\pi}{f_{rep}} f_{CE} \tag{1}$$

results in every n-th pulse being identical. For further amplification at kHz repetition rates, every (m·n)-th pulse is then picked out. By changing the nonlinear phase gathered by the pulse during each roundtrip, f_{CE} can be controlled. The pump power is usually chosen as the control variable, mediating nonlinear phase changes via the intracavity pulse intensity. The control loop on f_{CE} is generally closed using feedback based on a phase comparison. Such a phase-locked

* fabian.luecking@femtolasers.com

Ultrafast Phenomena and Nanophotonics XVI,
Edited by Markus Betz, Abdulhakem Y. Elezzabi, Jin-Joo Song, Kong-Thon Tsen,
Proc. of SPIE Vol. 8260, 82601A · © 2012 SPIE · CCC code: 0277-786X/12/$18 · doi: 10.1117/12.916186

loop (PLL) relies on deriving a phase difference φ between n^{-1} f_{rep} and f_{CE} and mapping it to a control voltage with limited range U_p, therefore fixing the product of sensitivity $dU/d\varphi$ and input error range $U(\varphi_{max}) = U_p$. This introduces a significant disadvantage, namely a trade-off between sensitivity and acceptable error range. Consequently, high stabilization performance makes the loop prone to drop-outs even at weak perturbations, whereas a reliable lock compromises precision. Because the feedback loop practically controls the intracavity energy, the laser will ideally exhibit reduced amplitude noise while locked. This positive side effect comes at the price that the control can just as well push the oscillator out of the regime of stable mode-locking in case of a perturbation. As this presents a great risk to subsequent amplification stages, the control loop gain is rarely pushed to its theoretical limits. Implicitly, this also affects the loop bandwidth, i.e., the upper limit to the frequency up to which noise on the CEO frequency can be corrected for. In real-world applications, this figure rarely exceeds some tens of kilohertz. Another limitation of the conventional scheme arises in experiments demanding a train of identical pulses at the full oscillator repetition rate[4,5], i.e. f_{CE}=0. The PLL relies on heterodyning, thus requiring the involved frequencies to be non-zero. This limitation can be circumvented[6], but the modified scheme requires an interferometer with non-common paths, thereby introducing additional noise. With respect to the current power scaling trends in laser development[7,8], another problem arises. Since the conventional scheme uses intracavity nonlinearities, it requires the use of soliton mode-locking. In addition, the pump source must provide both excellent power stability and modulation capability well above acoustic frequencies. Current power scaling concepts, drawing on high-power but low-brightness diode pumps, conflict with either or both of these prerequisites.

1.2 Feed-forward CEP stabilization

The feed-forward (FF) method[9] provides a solution to these issues. A frequency comb at arbitrary offset frequency is produced by subtracting f_{CE} from the free-running mode-locked laser in an acousto-optic frequency shifter (AOFS). Instead of controlling the intracavity CEO frequency, f_{CE} is measured and subsequently subtracted from the comb modes by interaction with the transient acoustic grating in a Bragg scattering process. As a cavity-external approach, it decouples generation of the pulse train from stabilization. Since no PLL is involved, the control is inherently robust. The bandwidth is determined primarily by the travelling time of the acoustic wave to the interaction region with the light. In theory, any laser frequency comb could be stabilized in this fashion, provided its CEO frequency can be measured. The initial demonstration of the feed-forward technique set a new benchmark. 45 mrad residual f_{CE} phase jitter (5 s measurement time, 0.2 Hz to 2.5 MHz) were achieved. However, the usability of the stabilized output was hampered by uncompensated angular chirp and the dispersion of the employed materials. The use of a photonic crystal fiber also limited the available power in the stabilized output to about 20 mW. A more recent publication[10] contains a comparison and combination of conventional and feed-forward stabilization, but the aforementioned issues have remained unsolved. In order to make a feed-forward stabilized laser suitable for amplifier seeding or direct use in CEP-sensitive experiments at the full repetition rate, the issues of power, pulse duration and beam quality have to be addressed.

2. EXPERIMENTAL SETUP

2.1 Experimental setup

Our setup is depicted in Fig. 1. A Ti:Sapphire oscillator (RAINBOW™, Femtolasers GmbH) serves as the source of few-cycle pulses, delivering 575 mW of average power in < 7 fs pulses at a repetition rate of 77 MHz. The CEO frequency of the free-running laser is measured in a monolithic in-loop (IL) interferometer[11], providing the signal $f_{CE,IL}$ with a 35 dB SNR (resolution bandwidth 100 kHz). This type of interferometer minimizes the influence of external noise sources because it is free of non-common paths and requires no delay line. Both broadening to an optical octave by self-phase modulation (SPM) and frequency mixing happen in the focus inside a periodically poled lithium niobate crystal and thus are narrowly confined in space and time. The frequency mixing processes can include both difference frequency generation and second harmonic generation, albeit a high spatial and temporal quality of the pulses is required to achieve suitable signal levels at the nanojoule level output of the oscillator. The CEO frequency beats can then be observed both in the green (530 nm, f-to-2f) as well as in the IR (1300 nm; 0-to-f) part of the spectrum. $f_{CE,IL}$ is low-pass filtered at 30 MHz and amplified before being mixed with a fixed frequency signal from an RF generator (f_{RF}) to reach the AOFS driving band (f_{AOFS}) of 85±1 MHz, i.e.,

$$f_{CE,IL} + f_{RF} = f_{AOFS}. \quad (2)$$

Note that setting f_{RF} to an integer multiple of the repetition rate results in zero CEP slip while obviating the need for an RF source [Eq. (1)]. A pair of chirped mirrors is used to pre-compensate the material dispersion of the setup. The pulses are weakly focused into the AOFS, which is placed at Bragg's angle for the -1st diffraction order. In addition to the frequency down-shift, the transient grating induced by the acoustic wave imprints a linear angular chirp that translates to spatial chirp at the point of recollimation. We correct the angular dependence by placing a BK7 prism (18° apex angle) directly behind the AOFS output facet. The prism is oriented such that the residual spatial chirp is minimized, which was verified by scanning the input facet of a fiber-coupled spectrometer over the collimated far-field beam profile. A diffraction efficiency of more than 75 % is achieved, corresponding to 175 mW of average power in the -1st diffraction order. At this point, a pulse duration of 9.8 fs was measured by interferometric second-order autocorrelation.

2.2 Out-of-loop measurement

The frequency-shifted pulses in the -1st diffraction order constitute a pulse train with arbitrary CEO frequency, as the frequency of every comb line was reduced by f_{AOFS} [Eq. (2)]:

$$\begin{aligned} f_{CE,OOL} &= f_{CE,IL} - f_{AOFS} \\ &= f_{CE,IL} - (f_{CE,IL} + f_{RF}) \\ &= -f_{RF} \end{aligned} \quad (3)$$

with $f_{CE,OOL}$ being the result of an out-of-loop (OOL) measurement. This step is performed in a second monolithic interferometer, resulting in a 30 dB beat signal. Heterodyning f_{RF} and $f_{CE,OOL}$ on a phase detector yields a DC signal, deviation from which represents phase noise between the target RF and the OOL measurement. After low-pass filtering at the Nyquist frequency f_N, the signal is recorded with a digital sampling oscilloscope at the maximum available memory size of 20 MSa. Voltage-to-phase calibration is obtained by replacing the OOL signal by a second RF source of equal power level fixed at a slightly different frequency. The linear phase evolution between the two yields a sine wave whose maxima indicate ± π/2 phase difference.

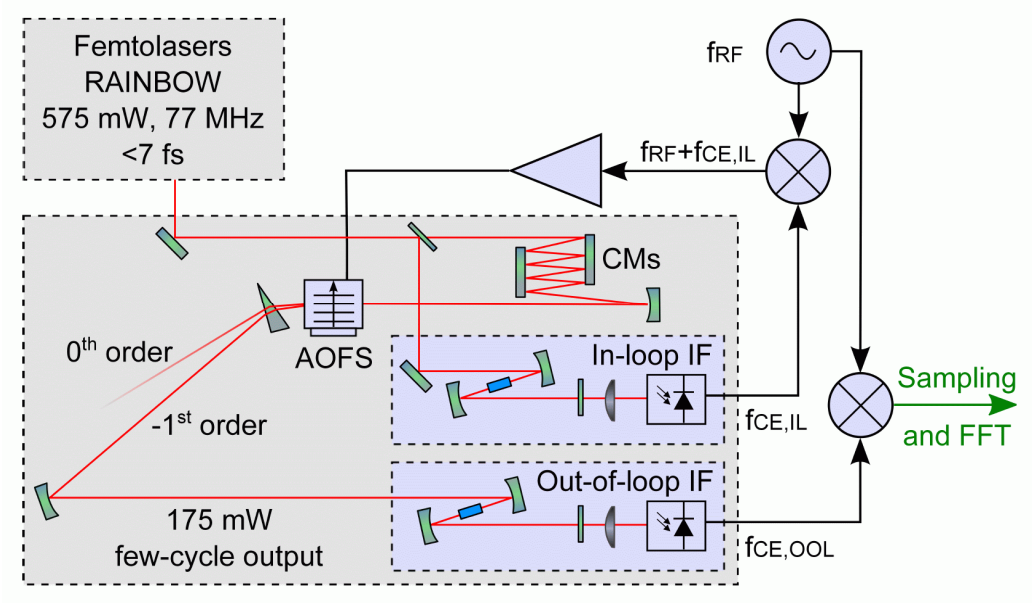

Figure 1. Schematic view of the experimental setup for phase noise characterization. IF, interferometer; CM, chirped mirror. Band-pass filters and preamplifiers have been omitted for reasons of clarity, angles are exaggerated.

3. PHASE NOISE MEASUREMENT

Short-term, mid-term and long-term measurements of the residual phase noise were made. The integrated RMS phase noise (IPN) is obtained by integration of noise power density over frequency:

$$\mathrm{IPN} = \left(\int_0^{f_N} [\mathrm{PND(f)}]^2 \, df \right)^{1/2} . \qquad (2)$$

In the 4 s time series (Fig. 2), IPN amounts 49 mrad. This value presents an upper limit to the actual phase error since detection shot noise masks the underlying noise signature. The exact contribution of detection shot noise to this figure cannot be directly measured, but based on the linearity and level of the noise density above 1 kHz, it can be safely assumed that the measured curve primarily shows shot noise except for the features around 1-2 MHz. The 20 s time series (Fig. 3) spans from the range of relaxation oscillations over the entire acoustic band down to the regime of environmental drifts. Still, shot noise remains the only significant contribution to an IPN of 30 mrad. At these longer timescales, the advantages of using inherently stable interferometers for CEO frequency detection become apparent, particularly in the 33 minute measurement (Fig. 4). The residual phase noise of 80 mrad compares favorably to the noise figure of 570 mrad obtained in [9], where the acoustic band is not even evaluated due to a high-frequency cut-off at 50 Hz. While acoustic perturbations and noise background contribute a mere 30 mrad to the IPN, about 50 mrad are due to a 1/f-like component, which we assume to be caused by the following mechanism. Due to ambient temperature or pressure changes, the CEO frequency of the free-running laser slowly drifts, changing $f_{CE,IL}$. With f_{RF} being fixed, $f_{AOFS} = f_{CE,IL} + f_{RF}$ gradually moves out of the filter pass-band at 85 MHz, allowing electronic noise to drive the power amplifier stage. This drift could be corrected using a slow feedback loop via intra-cavity wedges in order to keep the oscillator CEO frequency within a 1 MHz range. Alternatively, filters with a slightly broader pass-band could be used. However, even without any efforts made to correct the drift, the measured RMS phase error of 80 mrad over 33 minutes is, to the best of our knowledge, the lowest value ever reported over a comparable span of time.

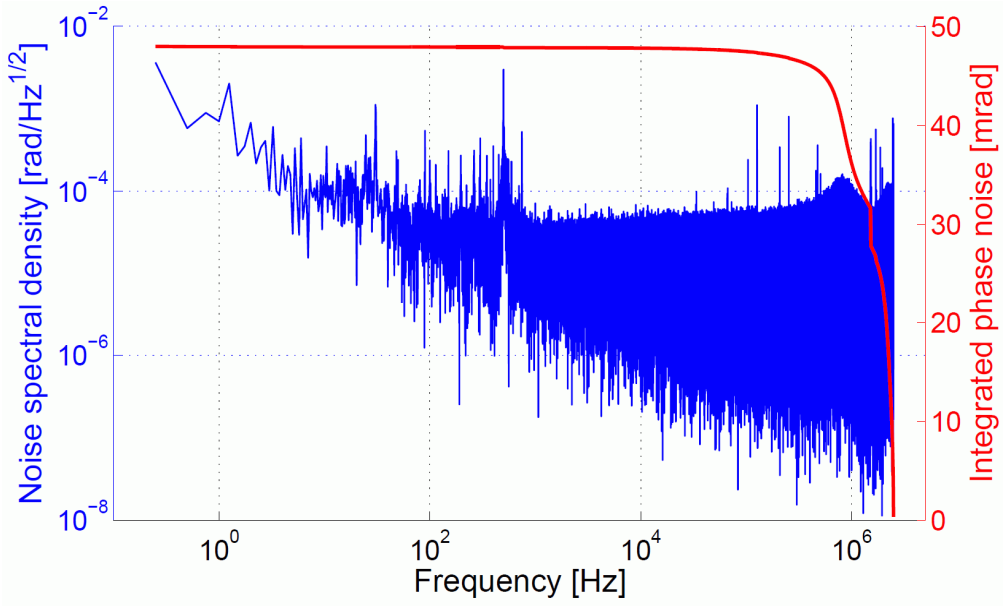

Figure 2. Frequency analysis of a short-term (4 s) phase noise time series covering the frequency range of 0.25 Hz to 2.5 MHz. *Blue curve*: phase noise density; *Red curve*: integrated phase noise (IPN). The step in the low megahertz range, possibly due to relaxation oscillations of the cavity, shows the approximate limit of the AOFS correction bandwidth.

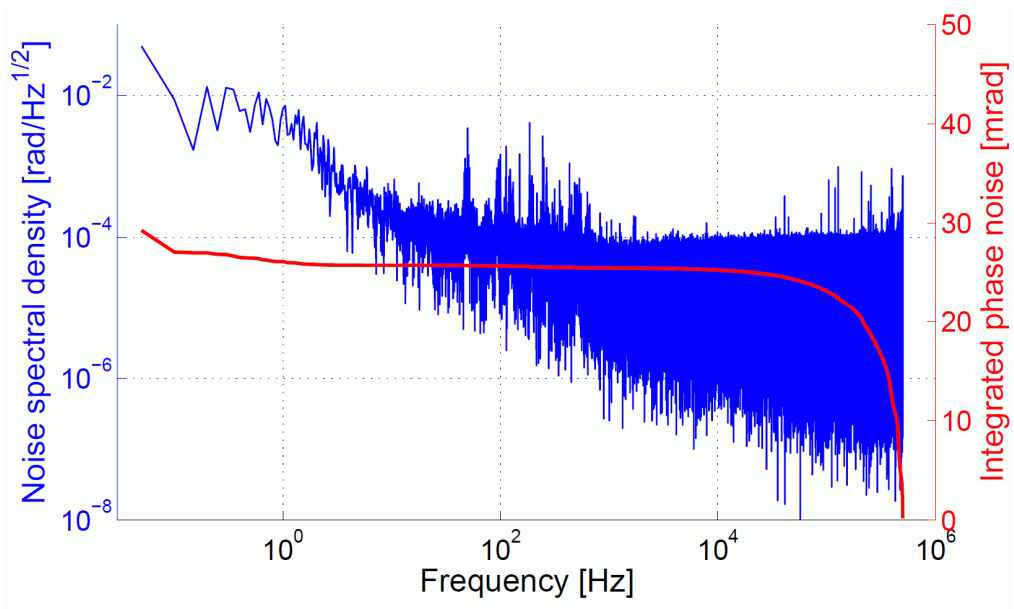

Figure 3. Frequency analysis of a mid-term (20 s) phase noise time series covering the frequency range of 50 mHz to 500 kHz. *Blue curve*: phase noise density; *Red curve*: integrated phase noise (IPN). Over the entire frequency range, shot noise remains the only visible contribution.

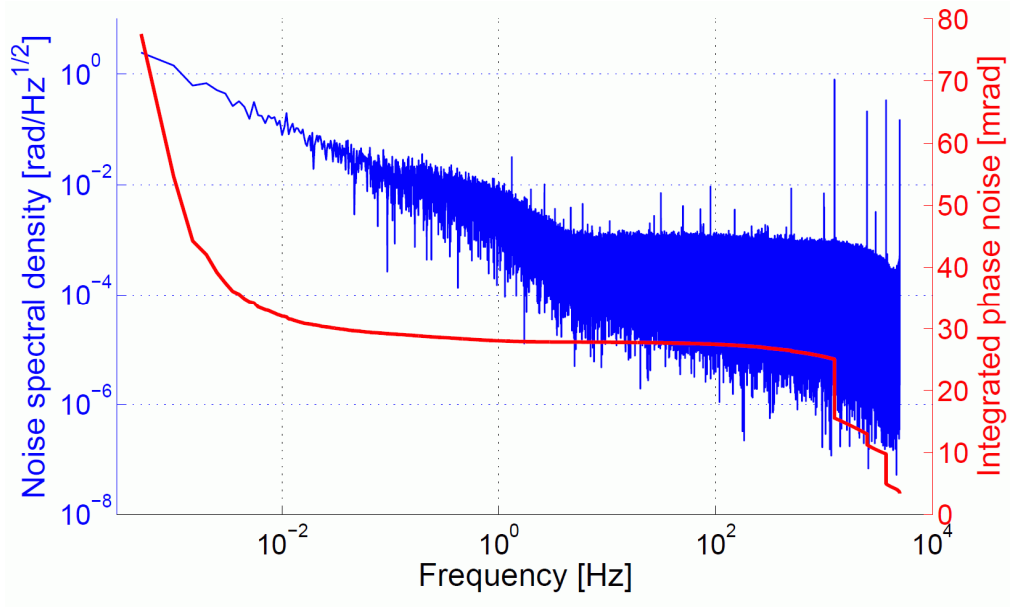

Figure 4. Frequency analysis of a long-term (33 minutes) phase noise time series covering the frequency range of 0.5 mHz to 5 kHz. *Blue curve*: phase noise density; *Red curve*: integrated phase noise (IPN). Three parts make up the IPN signature: Weak step-like features from acoustic perturbations in the kilohertz range, shot noise and a 1/f component at low frequencies (see text).

4. CONCLUSION

We have solved two issues preventing the use of feed-forward stabilization in seeding amplifier chains. We have removed spatial and temporal dispersion introduced by the AOFS, as demonstrated by efficient difference frequency generation in the out-of-loop interferometer. Using monolithic rather than fiber-based interferometers, we achieved excellent stabilization performance on significantly extended timescales. The long-term CEP stability of the present system makes it an ideal seed source for CEP-stabilized amplifiers and could obviate the need for a second slow loop in many applications. We believe that the performance of the feed-forward scheme highly simplifies sophisticated experiments in attosecond physics and may even enable applications currently deemed impossible due to the lack in precision and reliability of earlier CEP locking schemes.

5. OUTLOOK

As mentioned in the introduction, the FF stabilization scheme is applicable not only to current Ti:Sapphire systems, but also to alternative sources of few-cycle pulses. Power-scalable sources like thin-disk, slab and fiber lasers based on rare earth doped media have been shown to be suitable for the generation of microjoule pulses with some tens of femtoseconds duration[12,13]. Even shorter pulses at somewhat lower energies could be achieved using a chirped-pulse oscillator[14]. None of the sources used in these experiments could be CEP-stabilized using conventional methods, but the FF scheme could lend itself to this task. First proof-of-principle experiments have been performed with preliminary, yet promising results. Should these approaches prove feasible, attosecond science at megahertz repetition rate will have made a considerable step towards reality.

ACKNOWLEDGEMENTS

The authors acknowledge funding by the European Union through the Marie Curie network ATTOFEL (Grant Agreement No. 238362) as well as support from the Deutsche Forschungsgemeinschaft, Cluster of Excellence *Munich Centre for Advanced Photonics*.

REFERENCES

[1] Xu, L., Spielmann, C., Poppe, A., Brabec, T., Krausz, F. and Hänsch, T. W., "Route to phase control of ultrashort light pulses," Opt. Lett. 21, 2008-2010 (1996).

[2] Diddams, S. A., Jones, D. J., Ye, J., Cundiff, S. T., Hall, J. L., Ranka, J. K., Windeler, R. S., Holzwarth, R., Udem, T. and Hänsch, T. W., "Direct link between microwave and optical frequencies with a 300 THz femtosecond laser comb," Phys. Rev. Lett. 84, 5102-5105 (2000).

[3] Poppe, A., Holzwarth, R., Apolonski, A., Tempea, G., Spielmann, Ch., Hänsch, T. W. and Krausz, F., "Few-cycle optical waveform synthesis," Appl. Phys. B 72, 373-376 (2000).

[4] Wolf, A. L., Morgenweg, J., Koelemeij, J. C. J., van den Berg, S. A., Ubachs, W. and Eikema, K. S. E., "Direct frequency-comb spectroscopy of a dipole-forbidden clock transition in trapped ^{40}Ca+ ions," Opt. Lett. 36, 49-51 (2009)

[5] Kim, S.-C., Jin, J.-H., Kim, Y.-J., Park, I.-Y., Kim, Y.-S. and Kim, S.-W., "High-harmonic generation by resonant plasmon field enhancement," Nature 452, 757-760 (2008).

[6] Rausch, S., Binhammer, T., Harth, A., Schulz, E., Siegel, M. & Morgner, U., "Few-cycle oscillator pulse train with constant carrier-envelope- phase and 65 as jitter," Opt. Express 17, 20282-20290 (2009).

[7] Eidam, T., Hanf, S., Seise, E., Andersen, T. V., Gabler, T., Wirth, C., Schreiber, T., Limpert, J. and Tünnermann, A., "Femtosecond fiber CPA system emitting 830 W average output power," Opt. Lett. 35, 94-96 (2010).

[8] Russbüldt, P., Mans, T., Rotarius, G., Weitenberg, J., Hoffmann, H. D. and Poprawe, R., "400W Yb:YAG Innoslab fs-Amplifier," Opt. Express 17, 12230-12245 (2009).

[9] Koke, S., Grebing, C., Frei, H., Anderson, A., Assion, A. and Steinmeyer, G., "Direct frequency comb synthesis with arbitrary offset and shot-noise-limited phase noise," Nature Photonics 4, 462-465 (2010).

[10] Borchers, B., Koke, S., Husakou, A., Herrmann, J. and Steinmeyer, G., "Carrier-envelope phase stabilization with sub-10 as residual timing jitter," Opt. Lett. 36, 4146-4148 (2011).

[11] Fuji, T., Rauschenberger, J., Apolonski, A., Yakovlev, V. S., Tempea, G., Udem, T., Gohle, C., Hänsch, T. W., Lehnert, W., Scherer, M. and Krausz, F., "Monolithic carrier-envelope phase-stabilization scheme," Opt. Lett 30, 332-334 (2005).

[12] Vernaleken, A., Weitenberg, J., Sartorius, T., Russbueldt, P., Schneider, W., Stebbings, S. L., Kling, M. F., Hommelhoff, P., Hoffmann, H.-D., Poprawe, R., Krausz, F., Hänsch, T. W. and Udem, T., "Single-pass high-harmonic generation at 20.8 MHz repetition rate," Opt. Lett. 36, 3428-3430 (2011).

[13] Saraceno, C. J., Heckl, O. H., Baer, C. R. E., Südmeyer, T. and Keller, U., "Pulse compression of a high-power thin disk laser using rod-type fiber amplifiers," Opt. Express 19, 1395-1407 (2011).

[14] Ganz, T.; Pervak, V.; Apolonski, A. and Baum, P., "16 fs, 350 nJ pulses at 5 MHz repetition rate delivered by chirped pulse compression in fibers," Opt. Lett. 36, 1107-1109 (2011).